Interleukin-10 suppression enhances T-cell antitumor immunity and responses to checkpoint blockade in chronic lymphocytic leukemia

J.R. Rivas[1,2], S.S. Alhakeem[1,2], Y. Liu[3,4], J.M. Eckenrode[3], F. Marti[5], J.P. Collard[1,2], Y. Zhang[3,4], K.A. Shaaban[3,4], N. Muthusamy[6], G.C. Hildebrandt[1,2,7], R.A. Fleischman[2,7], L. Chen[2,8], J.S. Thorson[2,3,4], M. Leggas[2,3,4], S. Bondada[1,2,#]

[1]Dept. of Microbiology, Immunology and Molecular Genetics, University of Kentucky, Lexington, KY 40536

[2]Markey Cancer Center, University of Kentucky, Lexington, KY 40536

[3] Dept. of Pharmaceutical Sciences, University of Kentucky, Lexington, KY 40536

[4]Center for Pharmaceutical Research and Innovation, University of Kentucky, Lexington, KY 40536

[5]Dept. of Surgery, University of Kentucky, Lexington, KY 40536

[6]Dept. of Internal Medicine and Comprehensive Cancer Center, Ohio State University, Columbus, OH 43210

[7]Division of Hematology and Blood and Marrow Transplant, University of Kentucky, Lexington, KY 40536

[8]Dept. of Biostatistics, University of Kentucky, Lexington, KY 40536

Running title: Suppressing interleukin-10 improves immune checkpoint blockade

#Correspondence: Subbarao Bondada, University of Kentucky, 800 Rose St., 212 Combs Research Building, Lexington, KY 40536; e-mail: bondada@email.uky.edu

Phone number: 859-323-4705; Fax number: 859-257-9608

Manuscript word count: 3999 **Abstract word count:** 200

Number of Figures: 8 **Number of references:** 59

Keywords: CLL, immune checkpoint blockade, IL-10, antitumor immunity

Abstract:

T-cell dysfunction is a hallmark of B-cell Chronic Lymphocytic Leukemia (CLL). CLL cells downregulate T-cell responses by expressing regulatory molecules including programmed death ligand-1 (PD-L1) and Interleukin-10 (IL-10). Immune checkpoint blockade (ICB) aims to restore T-cell function by preventing the ligation of inhibitory receptors like PD-1, however most CLL patients do not respond well to this therapy. Thus, we investigated whether IL-10 suppression could enhance antitumor T-cell activity and improve responses to ICB. Since CLL IL-10 expression depends on Sp1, we utilized a novel, better tolerated mithramycin analogue, $MTM_{ox}32E$, to suppress CLL IL-10. We found $MTM_{ox}32E$ inhibited mouse and human CLL IL-10 production and maintained T-cell effector function. In the Eμ-Tcl1 mouse model, treatment reduced plasma IL-10 and CLL burden while it increased $CD8^+$ T-cell proliferation, effector and memory cell prevalence, and interferon-γ production. When combined with ICB, suppression of IL-10 improved responses to anti-PD-L1 as shown by a 4.5-fold decrease in CLL cell burden compared with anti-PD-L1 alone. Combination therapy also produced more interferon-γ^+, cytotoxic effector $KLRG1^+$, and memory $CD8^+$ T-cells, with fewer exhausted T-cells than ICB alone. Since current therapies for CLL do not target IL-10, this provides a novel strategy to increase the efficacy of T-cell-based immunotherapies.

Introduction:

B-cell Chronic Lymphocytic Leukemia (CLL) is a malignancy of $CD5^+CD19^+$ B-lymphocytes accompanied by severe immune dysfunction. In CLL, T-cells are an essential component of the microenvironment that play a controversial role in disease progression. Patient T-cells exhibit numerous functional defects that impede immunity but retain expression of molecules that aid CLL growth. CLL cells downregulate antitumor T-cell responses by expressing regulatory molecules including checkpoint ligands and anti-inflammatory cytokines like interleukin-10 (IL-10)(1-5). As a result, CLL patient T-cells show decreased proliferation after stimulation, increased inhibitory receptor expression, and cytoskeletal defects that impair immune synapse formation(1, 6, 7). These functional defects result in skewed T-cell subset distributions, altered T-cell metabolism, and increased pseudo-exhausted T-cells that contribute to immune dysfunction in CLL(1, 8). Immune suppression becomes a major complication for CLL patients, as the leading causes of morbidity and mortality are infections and secondary cancers(9). Since CLL is rarely curable, there is a need for new approaches to restore immunity.

Unfortunately, treatments aiming to reestablish T-cell functionality have experienced limited success in CLL patients(10). After repeated antigen stimulation, T-cells begin to express checkpoint ligand receptors such as programmed death-1 (PD-1) that decrease T-cell receptor sensitivity. Ligation of these receptors decrease $CD8^+$ T-cell antitumor immunity and result in T-cell exhaustion(1). Antibody-based immune checkpoint blockade (ICB) can upregulate T-cell activity by preventing the interaction between these inhibitory receptors and their ligands. Pembrolizumab (anti-PD-1) ICB was tested in high risk CLL patients, but only those with Richter's transformation responded(10). This suggests that additional mechanisms downregulate T-cell antitumor immunity. Even adoptively transferred anti-CD20 chimeric antigen receptor (CAR) T-

cells upregulate apoptosis and exhaustion genes in most CLL patients, resulting in a surprisingly low frequency of responders(11). Hence several studies are exploring combination therapies to improve responses to T-cell immunotherapy in CLL(12-14).

Since IL-10 is a well-known anti-inflammatory cytokine, we reasoned that CLL-derived IL-10 also suppresses host antitumor T-cell responses(3, 4). Members of the IL-10 cytokine family control immune responses in cancer, autoimmune conditions, and inflammatory diseases. Elevated IL-10 levels are correlated with more aggressive disease in CLL and a variety of other cancers(15, 16). On average, plasma IL-10 levels are higher in CLL patients than healthy donors, and those with increased IL-10 have a worse 3-year survival rate(15). Reduced DNA methylation at the IL-10 locus or polymorphisms that increase IL-10 production are also correlated with decreased survival in CLL(17, 18). Despite the importance of IL-10 in the microenvironment and improved antitumor responses with IL-10 blockade(19-21), blocking IL-10 is not yet approved for cancer therapy(22, 23). In our previous study, we found IL-10R$^{-/-}$ CD8^{+} T-cells were more effective at controlling CLL growth in the Eμ-TCL1 mouse model(4). Eμ-TCL1 mice express the oncogene T-cell leukemia 1 (TCL1) under the μ-enhancer and the VH promoter which leads to development of an aggressive CLL-like disease in 9 to 11 months(24). Like their human counterparts, these murine CLL cells secrete IL-10 in a BCR dependent manner, which can be inhibited by small molecules that interact with kinases and transcription factors downstream of the BCR(3-5).

Here we hypothesized inhibiting IL-10 would restore host antitumor responses and improve the efficacy of T-cell-based immunotherapy. We suppressed CLL-derived IL-10 by inhibiting Sp1, a transcription factor required for CLL IL-10 production(4), with a novel analog of mithramycin ($MTM_{ox}32E$) and compared this to an anti-IL-10 blocking antibody. $MTM_{ox}32E$ exhibits reduced toxicity and increased potency in other cancer models (Liu and Eckenrode et al, manuscript in preparation)(25). When combined with

anti-PD-L1, we show suppressing IL-10 in this manner reduces tumor burden and enhances T-cell functionality in mice over ICB alone. Thus, suppressing IL-10 could potentially be used to improve antitumor T-cell function in human CLL and other cancers with T-cell dysfunctionality.

Methods:

Human CLL samples

Patient blood was obtained with informed consent in accordance with the regulations of the Institutional Review Board of the University of Kentucky Research Foundation. Diagnosis of CLL was assigned by board-certified hematologists (Supplementary Table 1). Peripheral blood mononuclear cells (PBMCs) were isolated by Ficoll-Paque density centrifugation, then $CD45^+CD5^+CD19^+$ CLL cells and their expression of CD38, Zap70 and CD49d were evaluated by flow cytometry (antibodies in Supplementary Table 2) on an LSR II flow cytometer (BD Biosciences, Franklin Lakes, NJ). Mutational status of the expressed BCR was determined by PCR amplification from PBMC RNA and sequencing, as previously described(4).

Mice

Eμ-TCL1 (C57BL/6J background), NOD.SCID IL-2R$\gamma^{-/-}$ (NSG), and C57BL/6J mice were bred in house. Experimental groups were randomized by including both genders and mice were aged 8-12 weeks. Animals were treated according to the ethical standards of the University of Kentucky Institutional Animal Care and Use Committee (IACUC). Three to four million $CD19^+$ bead purified Eμ-TCL1 cells were adoptively transferred into NSG mice with or without primed $CD8^+$ T-cells at a ratio of 32:1 (CLL:T). CD19 sorts were performed with MojoSort Mouse Pan B Isolation Kit II (BioLegend, San Diego, CA) and CD8 sorts with Miltenyi's magnetic-activated cell sorting (MACS) CD8α+ T-cell Isolation Kit (Miltenyi Biotec, Bergisch Gladbach, Germany) according to the manufacturers' protocols. To prime $CD8^+$ T-cells, ten million Ficoll-Paque purified Eμ-TCL1 splenocytes (>90% $CD5^+CD19^+$) were adoptively transferred into C57BL/6J mice and ten days later T-cells were sorted from the spleen. Disease burden was monitored by sub-mental or sub-mandibular bleeding to determine $CD45^+CD5^+CD19^+$ frequency on

an LSR II flow cytometer (BD Biosciences) and $CD45^+$ cell count on a MACSQuant VYB Flow Cytometer (Miltenyi Biotec). Mice were treated with 12mg/kg $MTM_{ox}32E$ or vehicle (5% Kolliphor EL, 1% DMSO) by intravenous tail vein injection, 150μg/mouse anti-IL-10 (clone JES5-2A5, BioXCell, West Lebanon, NH), or 10mg/kg anti-PD-L1 or isotype control by intraperitoneal injection (clone B7-H1, BioXCell). Investigators were not blinded to treatment groups. When $CD5^+CD19^+$ cells comprised more than 70% of the peripheral blood, mice were euthanized along with controls. For *in vivo* proliferation, 1mg of BrdU in 100μL PBS was injected intraperitoneally three hours before euthanasia.

Cell culture

Eμ-TCL1 splenocytes, human CLL PBMCs (hCLL), and sorted T-cell subsets were cultured at $1x10^6$/mL in complete RPMI 1640 (cRPMI) media for 24 hours in 96 well plates. Concentrations of inhibitors and stimulants used are listed in the figure legends. $CD8^+$ T-cells were sorted from C57BL/6J spleens as above, and $CD4^+$ T-cells were sorted with Miltenyi's MACS CD4+ T-cell Isolation Kit (Miltenyi Biotec) according to the manufacturer's protocol. Anti-human or mouse IgM (Jackson ImmunoResearch, West Grove, PA), CpG (Integrated DNA Technologies, Coralville, IA), anti-mouse CD3 (BioLegend), anti-mouse CD28 (BioLegend) and MTM (Enzo Life Sciences, Farmingdale, NY) are commercially sourced, while $MTM_{ox}32E$ was synthesized in house (Liu and Eckenrode et al, manuscript in preparation). Secreted cytokines were measured with ELISA MAX Standard Set Mouse or Human kits according to the manufacturer's protocol (BioLegend). Cellular viability was determined by resazurin fluorescence after collecting supernatants for cytokine ELISAs. Cells were resuspended in 0.1mM resazurin (Sigma Aldrich, St. Louis, MO) in cRPMI, incubated four hours at 37°C, and fluorescence readings (ex:560nm, em:590nm) were recorded with a SpectraMax M5 plate reader (Molecular Devices, Sunnyvale, CA)(26).

Proliferation assays

CD8$^+$ cells were primed and sorted as above, then cultured at 0.75x10^6/mL in cRPMI for three days with soluble 10µg/mL anti-CD3 (BioLegend) and/or Ficoll-Paque purified Eµ-TCL1 splenocytes in flat-bottom 96-well plates. After this, cells were pulsed with 1µCi ^{3}H-thymidine (Perkin Elmer, Waltham, MA) or 10µM BrdU for four hours at 37°C. Counts from ^{3}H-thymidine incorporation were measured with a TopCount NXT Microplate Scintillation & Luminescence Counter (Perkin Elmer) and BrdU incorporation was measured on an LSR II flow cytometer (BD Biosciences).

Statistics

A priori power analysis was performed to determine the number of mice used in each experiment. GraphPad Prism 8 software was used to perform comparisons after completion (GraphPad Software, San Diego, CA). Tests used to determine statistical significance are listed in each figure legend. To determine statistical significance, one-way ANOVA was used for three or more groups, two-way ANOVA was used for two or more groups over various time points or concentrations, and two-tailed student's t-test was used between only two groups. Variance was comparable between groups in the same test.

Additional information is in the Supplementary Materials and Methods.

Results:

Blocking CLL-derived IL-10 restores T-cell function

Previously we observed removing IL-10 signaling from $CD8^+$ T-cells improves control of CLL growth in the Eμ-TCL1 adoptive transfer model(4). Considering IL-10 is a potent regulator of T-cell antitumor immunity(23), we hypothesized that CLL-derived IL-10 inhibits CLL-primed $CD8^+$ T-cell responses to antigenic stimuli. To test this, we primed C57BL/6J $CD8^+$ T-cells with Eμ-TCL1 splenocytes *in vivo* and determined their ability to respond to re-challenge with CLL *ex vivo*. Stimulation with anti-CD3 alone caused some T-cell proliferation, which was not changed by anti-IL-10 antibody (Figure 1A). In CLL-T-cell cocultures, IL-10 levels were only moderately increased, and anti-IL-10 did not change T-cell proliferation (Figures 1A, 1B). In contrast, at higher $CD8^+$:CLL ratios, proliferation increased four-fold when IL-10 was blocked (Figure 1A). This is not due to activity of anti-IL-10 on CLL cells, as blocking IL-10 does not enhance Eμ-TCL1 proliferation under co-culture conditions(4). Anti-CD3 activated $CD8^+$ T-cells produced a small amount of IL-10. IL-10 levels were much higher in CLL-$CD8^+$ T-cell co-cultures. (Figure 1B). In CLL-T-cell co-cultures there was very little IFN-γ which was substantially increased by neutralizing IL-10 Figure 1C).

In earlier studies we also showed CLL IL-10 production depends on Sp1 activity(4). Sp1 binds GC rich regions of DNA to regulate transcription, which can be competitively inhibited by MTM or MTM analogues(27). We observed that inhibiting CLL IL-10 with the MTM analogue $MTM_{ox}32E$ acted like the anti-IL-10 antibody in $CD8^+$:CLL co-cultures. CLL cells suppressed proliferation of primed CD8+ T-cells, which was rescued by $MTM_{ox}32E$ treatment in the 1:1 co-cultures, where high IL-10 levels were suppressed (Figure 1D). In 1:0.33 co-cultures, IL-10 levels were low with only a small effect of the drug on T-cell proliferation (Figure 1D-E). Drug treatment did not affect anti-CD3 driven proliferation of primed $CD8^+$ T-cells in isolation (Figure 1D). IL-10 levels

decreased with $MTM_{ox}32E$ treatment (Figure 1E), and IFN-γ secretion increased (Figure 1F), like in co-cultures blocked with anti-IL-10. Notably, 1μM $MTM_{ox}32E$ treatment did not alter IFN-γ secretion from anti-CD3 stimulated, primed $CD8^+$ T-cells in the absence of CLL (Figure 1F).

Novel MTM analogue suppresses IL-10 and preserves T-cell function

Dose response studies showed that $MTM_{ox}32E$ decreased Eμ-TCL1 IL-10 production with an IC50 of 70nM (Figure 2A). In contrast, $MTM_{ox}32E$ treatment did not significantly inhibit cytokine production by isolated $CD4^+$ or $CD8^+$ T-cells after 24 hours in culture (Figure 2A), or $CD8^+$ T-cell proliferation after 48 hours (Figure 2B) in the same dose range. $MTM_{ox}32E$ also decreased hCLL PBMC IL-10 production in 93% of patients tested (Figure 2C, Supplementary Table 3) and suppressed IL-10 production by the human CLL cell line, Mec-1 (Supplementary Figure 1A). Chromatin immunoprecipitation with Sp1 in Mec-1 cells showed $MTM_{ox}32E$ reduced Sp1 promoter occupancy of two GC rich sites in the IL-10 promoter (Figure 2D) and reduced IL-10 transcription (Supplementary Figure 1B), consistent with Sp1 displacement. Notably, the mRNA levels of Sp1 target genes involved in cell cycle and survival were less affected by $MTM_{ox}32E$ than MTM in Mec-1 cells and hCLL PBMCs, leading to less inhibition of cellular viability (Supplementary Figures 1B-E). $MTM_{ox}32E$ only mildly affected the viability of healthy human PBMCs after five days in culture (Supplementary Figure 1F) and did not decrease human $CD4^+$ and $CD8^+$ T-cell cytokine production in mixed cultures after 5 days at the dose (100nM) that blocks IL-10 production (Supplementary Figure 2), though there was some inhibition at higher doses (data not shown). Taken together, these results indicate $MTM_{ox}32E$ reduces CLL-derived IL-10 production while preserving antitumor T-cell activity.

Inhibiting CLL-derived IL-10 production enhances T-cell antitumor immunity

Since anti-IL-10 and $MTM_{ox}32E$ similarly suppressed CLL IL-10 and enhanced primed CD8+ T-cell activity in co-culture, these treatments were tested in our previously established adoptive transfer model of Eμ-TCL1 in NSG mice(4). Disease burden was monitored by the appearance of $CD5^+CD19^+$ CLL cells in the blood and mice were euthanized when blood CLL reached 70-80%. Without T-cells, CLL grew to 70-80% of peripheral blood cells in 15-16 days (Figure 2E-F, Supplementary Figures 3A, 4A). Transferring primed CD8+ T-cells at 1:32 ratio ($CD8^+$:CLL) significantly delayed the development of disease, and suppressing IL-10 further delayed disease development (Figure 2E-F). When mice were treated with anti-IL-10, leukemic burden is reduced in the blood (Figure 2E), spleen and bone marrow (Supplementary Figure 3B-C). Similarly, 12mg/kg $MTM_{ox}32E$ slowed disease progression in the blood, with less variability (Figure 2F). Both treatments reduced plasma IL-10 levels (Figures 2G-H), demonstrating that $MTM_{ox}32E$ can suppress CLL-derived IL-10 in mice, leading to decreased CLL burden.

Spleens from NSG mice also showed decreased CLL burden when IL-10 was suppressed with $MTM_{ox}32E$. Groups without T-cells had to be euthanized earlier due to faster CLL progression (day 17 versus day 22), so comparisons are made within T-cell and no T-cell groups. $MTM_{ox}32E$ treatment reduced CLL cell frequency in the spleen and bone marrow (Supplementary Figure 4B-D). However, splenic CLL burden (count) was only reduced in NSG mice given primed $CD8^+$ T-cells and $MTM_{ox}32E$ treatment (Figure 3A-B). The number of IL-10 producing splenic CLL cells (Figure 3C) and proliferative CLL cells in the spleen (Figure 3D) were also only reduced by IL-10 suppression when T-cells were present, indicating a requirement for T-cells. The lack of significance without T-cells may be because IL-10 does not affect CLL directly but inhibits the anti-CLL T-cell response. $CD8^+$ T-cells in blood and spleen were increased with anti-IL-10 blockade (Supplementary Figure 3D-E).

When IL-10 was suppressed with $MTM_{ox}32E$, $CD8^+$ T-cell functionality improved in Eμ-TCL1 recipient NSG mice. $CD8^+$ T-cells persisted throughout the experiment, with similar frequency and count in the blood and spleen but with a trend towards increase in the $MTM_{ox}32E$ group (Figure 4A, Supplementary Figure 4E-F). Like blocking IL-10 *in vitro*, $MTM_{ox}32E$ treatment increased $CD8^+$ T-cell proliferation as shown by increased number and frequency of splenic $BrdU^+CD5^+$ T-cells (Figure 4B). On average, the number and frequency of IFN-γ^+CD8^+ (Figure 4C) and Granzyme-B^+CD8^+ (GzB^+CD8^+) splenic T-cells (Figure 4D) increased with $MTM_{ox}32E$ treatment. Some mice upregulated cytokine production more than others. We found the mice with more proliferative T-cells also had more cytokine competent T-cells. With IL-10 suppression there was a more uniform increase in the frequency of $CD8^+$ cells expressing the effector T-cell marker, killer cell lectin-like receptor G1 (KLRG1), and the memory marker CD27 (Figure 4E). KLRG1+ effector T-cells are more cytotoxic and enhance protective immunity, and thus may be more active in control of CLL(28). Despite these changes, T-cells increased PD-1 expression with time, a marker of functionality and eventual exhaustion, regardless of drug treatment (Figure 4F). Therefore, we hypothesized anti-CLL immunity could be improved by combining IL-10 suppression with ICB.

Inhibiting CLL-derived IL-10 production improves responses to anti-PD-L1 checkpoint blockade

Previous reports described ICB reducing CLL burden in Eμ-TCL1 mice, especially in combination with other therapies(13, 29). Our results were similar, where anti-PD-L1 ICB alone modestly reduced CLL prevalence in the blood, and bone marrow but not spleen (Supplementary Figure 5A-D). Although there were more proliferating $CD8^+$ T-cells in spleen (Supplementary Fig 5E), ICB did not alter T-cell abundance, and yielded fewer IFN-γ^+ and more PD-1^+CD8^+ T-cells (Supplementary Figure 5F-G). We

designed our study to test whether IL-10 suppression could enhance the efficacy of anti-PD-L1 ICB in NSG mice given Eμ-TCL1 and primed $CD8^+$ T-cells.

With anti-PD-L1 ICB and $MTM_{ox}32E$ mediated IL-10 suppression combined (Supplementary Figure 6A), antitumor $CD8^+$ T-cells were more effective at controlling Eμ-TCL1. Combination therapy slowed CLL growth in the blood compared to anti-PD-L1 alone or isotype plus vehicle treated control mice (Figure 5A). By the end of the experiment, CLL frequency (Figure 5B) and burden (Figure 5C) in the spleen were on average 4.5-fold lower in combination therapy mice versus anti-PD-L1 alone (68.9% vs 15.4%; $94.9x10^6$ vs $21.1x10^6$ cells). In the spleen, the frequency and number of $CD8^+$ T-cells more than doubled (combination vs ICB: 6.97% vs 15.4%, $9.81x10^6$ vs $22.14x10^6$ cells, Figure 5D). $CD8^+$ T-cell levels in the blood were also elevated with combination therapy (Figure 5E, Supplementary Figure 6B). Spleen size was not different between the therapy groups, partially due to the expansion of T-cells with combination therapy (Supplementary Figure 6C-D). Furthermore, combination therapy reduced CLL spread to the bone marrow (1.58% vs 0.28%, $1.6x10^5$ vs $0.2x10^5$, Figure 5F). Combining ICB and IL-10 suppression dramatically altered the establishment of disease, as only one mouse receiving combination therapy developed more than 30% CLL in the blood by the end of the experiment (Figure 5G).

Adding IL-10 suppression to ICB altered the proliferative capacity of both CD8+ T-cells and CLL cells in NSG mice. As expected, $PD\text{-}L1^+$ CLL cells were decreased with ICB treatment (Figure 6A). Plasma IL-10 levels were lowest in mice receiving combination therapy, with intermediate IL-10 levels for anti-PD-L1 alone (Figure 6B). The number of $BrdU^+CD8^+$ T-cells were elevated in both groups (Figure 6C), but the number of dividing CLL cells only decreased with combination therapy (Figure 6D). This resulted in a greatly elevated ratio of total and proliferative $CD8^+$ to CLL cells with combination therapy (Figure 6E). Interestingly, plasma IL-10 levels inversely correlated

with the number of total and dividing $CD8^+$ T-cells, suggesting IL-10 plays a role in decreasing T-cell persistence and proliferation (Figure 6F).

When combining IL-10 suppression and ICB therapy, the outcome of T-cell activation was altered. $MTM_{ox}32E$ treatment increased the proportion of highly cytotoxic effector T-cells ($KLRG1^+$) and memory T-cells ($CD27^+$) over ICB alone (Figure 7A). There were also higher numbers of splenic IFN-γ^+CD8^+ and GzB^+CD8^+ T-cells (Figure 7B-C), and $CD8^+$ T-cells expressing CD107a, a marker of degranulation, in treated mice (Figure 7D). Still, similar levels of PD-1^+CD8^+ T-cells were detected in the blood throughout the experiment (Supplementary Figure 7A). PD-1 is upregulated after T-cell activation, and truly exhausted T-cells often express other exhaustion markers in addition to PD-1 (Figure 7E). Though there was a higher frequency of splenic PD-1^+CD8^+ T-cells in combination therapy mice (Figure 7F), very few $CD8^+$ T-cells expressed other markers of exhaustion, such as CTLA4, Lag3 or Tim-3 (Supplementary Figure 7B). The total frequency of exhausted cells (PD-1^+CTLA4^+, PD-1^+Lag3^+, or PD-$1^+Tim\text{-}3^+$) decreased for both treatment groups (Figure 7G, Supplementary Figure 7C), suggesting that most of the PD-1+ T-cells were not yet exhausted.

The increase in T-cell functionality with IL-10 suppression and ICB combination therapy shows clearly enhanced antitumor immunity compared to ICB alone, so lastly, we compared CLL burden within the previous experiment. With this comparison, the additive effect of IL-10 suppression and ICB became clear. CLL frequency is markedly lower in the spleen (Figure 7H) and blood (Figure 7I) with the combination therapy compared to either control or monotherapy. Taken together, these data show improved $CD8^+$ T-cell antitumor immunity in CLL with combined ICB and IL-10 suppression.

Discussion:

IL-10 downregulates $CD8^+$ antitumor immunity(4), and the therapeutic suppression of IL-10 enhanced $CD8^+$ T-cell control of CLL in these studies. However, CD8 T-cell PD-1 expression still increased with disease burden, therefore we combined IL-10 suppression with anti-PD-L1 ICB. This combination reduced disease burden compared to ICB alone and increased the number of $CD8^+$ T-cells, suggesting improved persistence. The numbers of $CD8^+$ T-cells expressing functional markers like IFN-γ, GzB, CD27, and KLRG1 increased and exhausted $CD8^+$ T-cells decreased, demonstrating a changed outcome of T-cell activation. These data show IL-10 suppression can improve T-cell functionality, antitumor immunity, and responses to ICB in CLL. They point to IL-10 suppression as a novel therapeutic strategy that may improve responses to T-cell-based immunotherapy in human CLL.

We describe $MTM_{ox}32E$, a novel small molecule inhibitor of CLL cell IL-10 production, which does not inhibit effector T-cell function, and enhances anti-CLL $CD8^+$ T-cell activity. $MTM_{ox}32E$ treatment reduced Sp1 occupancy of the IL-10 promoter and CLL IL-10 secretion but is uniquely less toxic than MTM. Like MTM, $MTM_{ox}32E$ interacts with GC rich regions of DNA. The keto group in the 3-C position in MTM is modified to an oxime group with methyl indolyl substitution, which may change its interactions with Sp1 or other GC box-binding proteins, (Yang et al manuscript in preparation) altering its tolerability. $MTM_{ox}32E$ treatment showed some selectivity for inhibiting Sp1 binding on the IL-10 promoter in cell culture. This may be due to interactions between the analogue and additional proteins in the transcription complex promoting CLL IL-10 production, which requires further investigation. $MTM_{ox}32E$ also has a small inhibitory effect on CLL growth in vivo but not in vitro when used as single agent. This could be due to its effect on the microenvironment, which also requires further investigation. Sp1 positively regulates murine T-BET (T-box expressed in T-cells), which controls natural killer and T-

cell IFN-γ expression, and MTM treatment reduced both T-BET and IFN-γ production in natural killer cells(30). However, Sp1 expression and transcriptional activity was shown to be upregulated in activated and proliferating $CD4^+$ T cells(31, 32), but not in activated $CD8^+$ T-cell subsets(33, 34). Our studies focused on $CD8^+$ T-cells, where we see no detrimental effect of $MTM_{ox}32E$ treatment. Additional studies are required to elucidate the differential effects of MTM and $MTM_{ox}32E$ on T-cells.

In CLL and several solid tumors, IL-10 reduced the inflammatory state of immune responses including $CD8^+$ T cells(23, 35-37), although there are examples where IL-10 supported antitumor T-cell function(38-40). Indeed, the role of IL-10 in cancer may be context dependent. In liver and prostate cancers IL-10 was shown to inhibit cytotoxic T-cell function and anti-cancer immunity(41, 42). The dose and duration of IL-10 exposure is critical to its regulatory effects on $CD8^+$ T-cell maturation into functional memory cells(43). The IL-10 pathway also plays a role in T-cell exhaustion during chronic viral infection, and can directly downregulate $CD8^+$ T-cell function(44, 45). Blocking IL-10 and PD-1 during chronic viral infection synergistically enhanced viral control and reversed $CD8^+$ T-cell exhaustion(46). Furthermore, we previously showed IL-10 inhibits macrophage pro-inflammatory cytokine secretion in the aged, which may be important as CLL mainly affects older individuals(47). $CD138^+PD\text{-}L1^+$ plasma cell derived IL-10 also affects immune responses to infectious agents in part by inhibiting innate immune cells(48). These innate cells and stromal cells are part of the microenvironment which supports CLL cell growth. Thus, regulation of innate cells by IL-10 may also contribute to the benefits from IL-10 suppression.

Expression of IL-10 by CLL cells is upregulated by B-cell receptor (BCR) signaling and may be reduced by inhibitors of this pathway. Many therapeutics for CLL inhibit kinases in BCR signaling(49, 50), and have yielded great clinical outcomes for CLL patients. The ability of Bruton's tyrosine kinase (Btk) inhibitors (i.e. ibrutinib) and

phosphoinoside-3 kinase (PI3K) inhibitors (i.e. idelalisib) to inhibit CLL growth are well studied, and may also enhance immune responses(51). However, some patients can develop resistance mutations or have worse disease after treatment cessation(52, 53). Ibrutinib treatment also affects T-cells, enhancing their function in CLL patients, which may be explained by reduced CLL-derived IL-10 in addition to its direct effects(54). $CD8^+$ T-cells in hCLL exist in a pseudo-exhausted state(8), and T-cell exhaustion may occur within certain T-cell populations in patients(55). Reversing this exhaustion may be possible with the right therapeutic strategy(56). In mouse studies blocking the PD-1/PD-L1 pathway was promising, but was more effective with additional blockade of Lag-3 or Tim-3(29, 57). Anti-PD-1 ICB primarily affects CD8+ T-cells and can rescue exhausted T-cells, in contrast with anti-CTLA4(58). Nivolumab (anti-PD-1) is currently in clinical trials for human CLL in combination with the Btk inhibitor ibrutinib (NCT02420912) since previous reports suggested this combination would be more effective than monotherapy(12-14). Our findings suggest combining PD-1/PD-L1 blockade with IL-10 suppression could also improve antitumor T-cell responses (Figure 8) and may still be effective for patients who have developed resistance to Btk inhibitors.

With no known cure and the number of cases increasing(59), there is a need for novel therapies for CLL. Heterogeneous responses to therapy make testing new strategies challenging(50). However, decreasing IL-10 to improve antitumor immunity provides an opportunity to overcome CLL-induced immunosuppression and enhance current CLL immunotherapies. Immune evasion through T-cell suppression is common to many types of cancer, so this strategy may also be applicable to other tumors(16, 19, 20, 22, 36). Further studies will reveal whether suppressing IL-10 will be an effective in treating human cancer patients.

Acknowledgements:

We would like to thank the patients and their families for participating in our research and Dr. Eric Durbin with the Kentucky Cancer Registry. We also thank Dr. Siva Gandhapudi and Dylan Rivas for their helpful discussion. Jacqueline R. Rivas is a Fellow of the Leukemia & Lymphoma Society.

The project described was supported in part by the National Center for Research Resources and the National Center for Advancing Translational Sciences, National Institutes of Health, through grants UL1TR001998 and UL1TR000117. It was also supported by the National Cancer Institute Cancer Center Support Grant P30CA177558, Training Grant T32CA165990 and Research Grants R01CA165469, R01CA217255, and R01CA217934. This research was supported by the Flow Cytometry and Immune Monitoring Shared Resource Facility of the University of Kentucky Markey Cancer Center (P30CA177558). The content is solely the responsibility of the authors and does not necessarily represent the official views of the NIH.

Competing Interests:

J.S.T. is a co-founder of Centrose (Madision, WI, USA). No other authors have competing financial interests.

References:

1. Brusa D, Serra S, Coscia M, Rossi D, D'Arena G, Laurenti L, et al. The PD-1/PD-L1 axis contributes to T-cell dysfunction in chronic lymphocytic leukemia. Haematologica. 2013;98(6):953-63.

2. McClanahan F, Riches JC, Miller S, Day WP, Kotsiou E, Neuberg D, et al. Mechanisms of PD-L1/PD-1-mediated CD8 T-cell dysfunction in the context of aging-related immune defects in the Emicro-TCL1 CLL mouse model. Blood. 2015;126(2):212-21.

3. DiLillo DJ, Weinberg JB, Yoshizaki A, Horikawa M, Bryant JM, Iwata Y, et al. Chronic lymphocytic leukemia and regulatory B cells share IL-10 competence and immunosuppressive function. Leukemia. 2013;27(1):170-82.

4. Alhakeem SS, McKenna MK, Oben KZ, Noothi SK, Rivas JR, Hildebrandt GC, et al. Chronic Lymphocytic Leukemia-Derived IL-10 Suppresses Antitumor Immunity. J Immunol. 2018;200(12):4180-9.

5. Alhakeem SS, Sindhava VJ, McKenna MK, Gachuki BW, Byrd JC, Muthusamy N, et al. Role of B cell receptor signaling in IL-10 production by normal and malignant B-1 cells. Ann N Y Acad Sci. 2015;1362:239-49.

6. Ramsay AG, Johnson AJ, Lee AM, Gorgun G, Le Dieu R, Blum W, et al. Chronic lymphocytic leukemia T cells show impaired immunological synapse formation that can be reversed with an immunomodulating drug. J Clin Invest. 2008;118(7):2427-37.

7. Palma M, Gentilcore G, Heimersson K, Mozaffari F, Nasman-Glaser B, Young E, et al. T cells in chronic lymphocytic leukemia display dysregulated expression of immune checkpoints and activation markers. Haematologica. 2017;102(3):562-72.

8. Riches JC, Davies JK, McClanahan F, Fatah R, Iqbal S, Agrawal S, et al. T cells from CLL patients exhibit features of T-cell exhaustion but retain capacity for cytokine production. Blood. 2013;121(9):1612-21.

9. Forconi F, Moss P. Perturbation of the normal immune system in patients with CLL. Blood. 2015;126(5):573-81.

10. Ding W, LaPlant BR, Call TG, Parikh SA, Leis JF, He R, et al. Pembrolizumab in patients with CLL and Richter transformation or with relapsed CLL. Blood. 2017;129(26):3419-27.

11. Fraietta JA, Lacey SF, Orlando EJ, Pruteanu-Malinici I, Gohil M, Lundh S, et al. Determinants of response and resistance to CD19 chimeric antigen receptor (CAR) T cell therapy of chronic lymphocytic leukemia. Nat Med. 2018;24(5):563-71.

12. Freeman CL, Gribben JG. Immunotherapy in Chronic Lymphocytic Leukaemia (CLL). Curr Hematol Malig Rep. 2016;11(1):29-36.

13. Sagiv-Barfi I, Kohrt HE, Czerwinski DK, Ng PP, Chang BY, Levy R. Therapeutic antitumor immunity by checkpoint blockade is enhanced by ibrutinib, an inhibitor of both BTK and ITK. Proc Natl Acad Sci U S A. 2015;112(9):E966-72.

14. Fraietta JA, Beckwith KA, Patel PR, Ruella M, Zheng Z, Barrett DM, et al. Ibrutinib enhances chimeric antigen receptor T-cell engraftment and efficacy in leukemia. Blood. 2016;127(9):1117-27.

15. Fayad L, Keating MJ, Reuben JM, O'Brien S, Lee BN, Lerner S, et al. Interleukin-6 and interleukin-10 levels in chronic lymphocytic leukemia: correlation with phenotypic characteristics and outcome. Blood. 2001;97(1):256-63.

16. Zhao S, Wu D, Wu P, Wang Z, Huang J. Serum IL-10 Predicts Worse Outcome in Cancer Patients: A Meta-Analysis. PLoS One. 2015;10(10):e0139598.

17. Dai ZM, He AL, Zhang WG, Liu J, Cao XM, Chen YX, et al. Association of the four common polymorphisms in interleukin-10 (rs1800890, rs1800896, rs1800871, and rs1800872) with non-Hodgkin's lymphoma risk: a meta-analysis. Int J Clin Exp Med. 2014;7(12):4720-33.

18. Drennan S, D'Avola A, Gao Y, Weigel C, Chrysostomou E, Steele AJ, et al. IL-10 production by CLL cells is enhanced in the anergic IGHV mutated subset and associates with reduced DNA methylation of the IL10 locus. Leukemia. 2017.

19. Lamichhane P, Karyampudi L, Shreeder B, Krempski J, Bahr D, Daum J, et al. IL10 Release upon PD-1 Blockade Sustains Immunosuppression in Ovarian Cancer. Cancer Res. 2017;77(23):6667-78.

20. Gordy JT, Luo K, Francica B, Drake C, Markham RB. Anti-IL-10-mediated Enhancement of Antitumor Efficacy of a Dendritic Cell-targeting MIP3alpha-gp100 Vaccine in the B16F10 Mouse Melanoma Model Is Dependent on Type I Interferons. J Immunother. 2018;41(4):181-9.

21. Wu X, Hsu DK, Wang KH, Huang Y, Mendoza L, Zhou Y, et al. IL-10 is overexpressed in human cutaneous T-cell lymphoma and is required for maximal tumor growth in a mouse model. Leuk Lymphoma. 2019;60(5):1244-52.

22. Sato T, Terai M, Tamura Y, Alexeev V, Mastrangelo MJ, Selvan SR. Interleukin 10 in the tumor microenvironment: a target for anticancer immunotherapy. Immunol Res. 2011;51(2-3):170-82.

23. Oft M. IL-10: master switch from tumor-promoting inflammation to antitumor immunity. Cancer Immunol Res. 2014;2(3):194-9.

24. Bichi R, Shinton SA, Martin ES, Koval A, Calin GA, Cesari R, et al. Human chronic lymphocytic leukemia modeled in mouse by targeted TCL1 expression. Proc Natl Acad Sci U S A. 2002;99(10):6955-60.

25. Hou C, Weidenbach S, Cano KE, Wang Z, Mitra P, Ivanov DN, et al. Structures of mithramycin analogues bound to DNA and implications for targeting transcription factor FLI1. Nucleic Acids Res. 2016;44(18):8990-9004.

26. Mitra P, Eckenrode JM, Mandal A, Jha AK, Salem SM, Leggas M, et al. Development of Mithramycin Analogues with Increased Selectivity toward ETS Transcription Factor Expressing Cancers. J Med Chem. 2018;61(17):8001-16.

27. Choi ES, Nam JS, Jung JY, Cho NP, Cho SD. Modulation of specificity protein 1 by mithramycin A as a novel therapeutic strategy for cervical cancer. Sci Rep. 2014;4:7162.

28. Herndler-Brandstetter D, Ishigame H, Shinnakasu R, Plajer V, Stecher C, Zhao J, et al. KLRG1(+) Effector CD8(+) T Cells Lose KLRG1, Differentiate into All Memory T Cell Lineages, and Convey Enhanced Protective Immunity. Immunity. 2018;48(4):716-29 e8.

29. Wierz M, Pierson S, Guyonnet L, Viry E, Lequeux A, Oudin A, et al. Dual PD1/LAG3 immune checkpoint blockade limits tumor development in a murine model of chronic lymphocytic leukemia. Blood. 2018;131(14):1617-21.

30. Yu J, Wei M, Boyd Z, Lehmann EB, Trotta R, Mao H, et al. Transcriptional control of human T-BET expression: the role of Sp1. Eur J Immunol. 2007;37(9):2549-61.

31. Lacroix I, Lipcey C, Imbert J, Kahn-Perles B. Sp1 transcriptional activity is up-regulated by phosphatase 2A in dividing T lymphocytes. J Biol Chem. 2002;277(11):9598-605.

32. Juang YT, Rauen T, Wang Y, Ichinose K, Benedyk K, Tenbrock K, et al. Transcriptional activation of the cAMP-responsive modulator promoter in human T cells is regulated by protein phosphatase 2A-mediated dephosphorylation of SP-1 and reflects disease activity in patients with systemic lupus erythematosus. J Biol Chem. 2011;286(3):1795-801.

33. Moskowitz DM, Zhang DW, Hu B, Le Saux S, Yanes RE, Ye Z, et al. Epigenomics of human CD8 T cell differentiation and aging. Sci Immunol. 2017;2(8).

34. He B, Xing S, Chen C, Gao P, Teng L, Shan Q, et al. CD8(+) T Cells Utilize Highly Dynamic Enhancer Repertoires and Regulatory Circuitry in Response to Infections. Immunity. 2016;45(6):1341-54.

35. Ruffell B, Chang-Strachan D, Chan V, Rosenbusch A, Ho CM, Pryer N, et al. Macrophage IL-10 blocks CD8+ T cell-dependent responses to chemotherapy by suppressing IL-12 expression in intratumoral dendritic cells. Cancer Cell. 2014;26(5):623-37.

36. Mahipal A, Terai M, Berd D, Chervoneva I, Patel K, Mastrangelo MJ, et al. Tumor-derived interleukin-10 as a prognostic factor in stage III patients undergoing adjuvant treatment with an autologous melanoma cell vaccine. Cancer Immunol Immunother. 2011;60(7):1039-45.

37. Sawant DV, Yano H, Chikina M, Zhang Q, Liao M, Liu C, et al. Adaptive plasticity of IL-10(+) and IL-35(+) Treg cells cooperatively promotes tumor T cell exhaustion. Nat Immunol. 2019;20(6):724-35.

38. Gu T, De Jesus M, Gallagher HC, Burris TP, Egilmez NK. Oral IL-10 suppresses colon carcinogenesis via elimination of pathogenicCD4(+) T-cells and induction of antitumor CD8(+) T-cell activity. Oncoimmunology. 2017;6(6):e1319027.

39. Emmerich J, Mumm JB, Chan IH, LaFace D, Truong H, McClanahan T, et al. IL-10 directly activates and expands tumor-resident CD8(+) T cells without de novo infiltration from secondary lymphoid organs. Cancer Res. 2012;72(14):3570-81.

40. Santin AD, Hermonat PL, Ravaggi A, Bellone S, Pecorelli S, Roman JJ, et al. Interleukin-10 increases Th1 cytokine production and cytotoxic potential in human papillomavirus-specific CD8(+) cytotoxic T lymphocytes. J Virol. 2000;74(10):4729-37.

41. Shalapour S, Lin XJ, Bastian IN, Brain J, Burt AD, Aksenov AA, et al. Inflammation-induced IgA+ cells dismantle anti-liver cancer immunity. Nature. 2017;551(7680):340-5.

42. Shalapour S, Font-Burgada J, Di Caro G, Zhong Z, Sanchez-Lopez E, Dhar D, et al. Immunosuppressive plasma cells impede T-cell-dependent immunogenic chemotherapy. Nature. 2015;521(7550):94-8.

43. Cui W, Liu Y, Weinstein JS, Craft J, Kaech SM. An interleukin-21-interleukin-10-STAT3 pathway is critical for functional maturation of memory CD8+ T cells. Immunity. 2011;35(5):792-805.

44. Brooks DG, Trifilo MJ, Edelmann KH, Teyton L, McGavern DB, Oldstone MB. Interleukin-10 determines viral clearance or persistence in vivo. Nat Med. 2006;12(11):1301-9.

45. Smith LK, Boukhaled GM, Condotta SA, Mazouz S, Guthmiller JJ, Vijay R, et al. Interleukin-10 Directly Inhibits CD8(+) T Cell Function by Enhancing N-Glycan Branching to Decrease Antigen Sensitivity. Immunity. 2018;48(2):299-312 e5.

46. Brooks DG, Ha SJ, Elsaesser H, Sharpe AH, Freeman GJ, Oldstone MB. IL-10 and PD-L1 operate through distinct pathways to suppress T-cell activity during persistent viral infection. Proc Natl Acad Sci U S A. 2008;105(51):20428-33.

47. Chelvarajan RL, Liu Y, Popa D, Getchell ML, Getchell TV, Stromberg AJ, et al. Molecular basis of age-associated cytokine dysregulation in LPS-stimulated macrophages. J Leukoc Biol. 2006;79(6):1314-27.

48. Lino AC, Dang VD, Lampropoulou V, Welle A, Joedicke J, Pohar J, et al. LAG-3 Inhibitory Receptor Expression Identifies Immunosuppressive Natural Regulatory Plasma Cells. Immunity. 2018;49(1):120-33 e9.

49. Roberts AW, Davids MS, Pagel JM, Kahl BS, Puvvada SD, Gerecitano JF, et al. Targeting BCL2 with Venetoclax in Relapsed Chronic Lymphocytic Leukemia. N Engl J Med. 2016;374(4):311-22.

50. Jain N, O'Brien S. Targeted therapies for CLL: Practical issues with the changing treatment paradigm. Blood Rev. 2016;30(3):233-44.

51. Woyach JA, Johnson AJ, Byrd JC. The B-cell receptor signaling pathway as a therapeutic target in CLL. Blood. 2012;120(6):1175-84.

52. Jain P, Thompson PA, Keating M, Estrov Z, Ferrajoli A, Jain N, et al. Long-term outcomes for patients with chronic lymphocytic leukemia who discontinue ibrutinib. Cancer. 2017;123(12):2268-73.

53. Ahn IE, Underbayev C, Albitar A, Herman SE, Tian X, Maric I, et al. Clonal evolution leading to ibrutinib resistance in chronic lymphocytic leukemia. Blood. 2017;129(11):1469-79.

54. Long M, Beckwith K, Do P, Mundy BL, Gordon A, Lehman AM, et al. Ibrutinib treatment improves T cell number and function in CLL patients. J Clin Invest. 2017;127(8):3052-64.

55. Hanna BS, Roessner PM, Yazdanparast H, Colomer D, Campo E, Kugler S, et al. Control of chronic lymphocytic leukemia development by clonally-expanded CD8(+) T-cells that undergo functional exhaustion in secondary lymphoid tissues. Leukemia. 2019;33(3):625-37.

56. Bachireddy P, Hainz U, Rooney M, Pozdnyakova O, Aldridge J, Zhang W, et al. Reversal of in situ T-cell exhaustion during effective human antileukemia responses to donor lymphocyte infusion. Blood. 2014;123(9):1412-21.

57. Ngiow SF, von Scheidt B, Akiba H, Yagita H, Teng MW, Smyth MJ. Anti-TIM3 antibody promotes T cell IFN-gamma-mediated antitumor immunity and suppresses established tumors. Cancer Res. 2011;71(10):3540-51.

58. Wei SC, Anang NAS, Sharma R, Andrews MC, Reuben A, Levine JH, et al. Combination anti-CTLA-4 plus anti-PD-1 checkpoint blockade utilizes cellular mechanisms partially distinct from monotherapies. Proc Natl Acad Sci U S A. 2019;116(45):22699-709.

59. Chen Q, Jain N, Ayer T, Wierda WG, Flowers CR, O'Brien SM, et al. Economic Burden of Chronic Lymphocytic Leukemia in the Era of Oral Targeted Therapies in the United States. J Clin Oncol. 2017;35(2):166-74.

Figure Legends:

Figure 1: CLL IL-10 suppresses T-cell responses. (A) Proliferation of CLL-primed $CD8^+$ T-cells in response to anti-CD3 or varying numbers of Eμ-TCL1 splenocytes after 72 hour stimulation, with or without 10μg/mL anti-IL-10. Secreted IL-10 (B) and IFN-γ (C) from cultures in panel A (Eμ-TCL1 spleen cells alone produced 986pg/mL IL-10 and 80pg/mL IFN-γ). (D) Proliferation of CLL-primed $CD8^+$ T-cells stimulated with anti-CD3 or varying numbers of Eμ-TCL1 splenocytes after 72 hours with or without 1μM $MTM_{ox}32E$. Secreted IL-10 (E) and IFN-γ (F) from cultures in panel D (Eμ-TCL1 spleen cells alone produced 948pg/mL IL-10 and 78pg/mL IFN-γ). Two-way ANOVA between control and antibody or inhibitor treatment was used to calculate statistical significance. **p<0.01, ***p<0.001, ****p<0.0001

Figure 2: $MTM_{ox}32E$ suppresses CLL IL-10 and anti-IL-10 enhances anti-CLL activity of T-cells. (A) Secreted IL-10 from Eμ-TCL1 splenocytes, IL-2 from murine C57BL/6 $CD4^+$ T-cells, and IFN-γ from murine C57BL/6 $CD8^+$ T-cells cultured for 24 hours with $MTM_{ox}32E$, normalized to vehicle control (660pg/mL, 398pg/mL, 106pg/mL, respectively). T-cells were stimulated with 10μg/mL anti-CD3. (B) Proliferation (BrdU incorporation) of C57BL/6 $CD8^+$ T-cells cultured for 72 hours with 10μg/mL anti-CD3 $\pm$ $MTM_{ox}32E$. (C) Secreted IL-10 from human CLL PBMCs stimulated with 25μg/mL anti-IgM for 24 hours with $MTM_{ox}32E$, normalized to vehicle control (17-656pg/mL). (D) Promoter occupancy of Sp1 GC-rich sites on the human IL-10 promoter in Mec1 cells treated with 1000nM $MTM_{ox}32E$. (E-F) Frequency of Eμ-TCL1 CLL cells in the blood of NSG mice (mean + SEM). Six groups of eight NSG mice were injected with Eμ-TCL1 CLL, with or without Eμ-TCL1 primed $CD8^+$ T-cells (CLL to T cell ratio of 32:1) and received 150μg anti-IL-10 or isotype every two days (E) or 12mg/kg $MTM_{ox}32E$ or

vehicle every three days (F). Stars indicate statistical significance of differences between control and anti-IL-10 (E) or $MTM_{ox}32E$ (F) treated group. (G-H) Plasma IL-10 levels in NSG mice from E-F (mean + SEM). Stars indicate significance between control and anti-IL-10 (G) or $MTM_{ox}32E$ (H) treated group. Statistical comparisons in A and E-H were performed with two-way ANOVA comparing all groups to each other, and in D one-way ANOVA for vehicle to $MTM_{ox}32E$ at each GC-rich site. *p<0.05, **p<0.01, ***p<0.001, VC=vehicle control

Figure 3: Inhibiting CLL IL-10 with $MTM_{ox}32E$ requires T-cells for optimal effect. Four groups of eight NSG mice were injected with Eμ-TCL1 CLL, with or without Eμ-TCL1 primed $CD8^+$ T-cells (CLL:T cell ratio 32:1) and received 12mg/kg $MTM_{ox}32E$ or vehicle every three days. (A) Gating strategy for detecting CLL cells, IL-10 production, and BrdU incorporation. (B) Burden of Eμ-TCL1 CLL cells in the spleen of NSG mice without $CD8^+$ T-cells (left panel, euthanized day 17) and with $CD8^+$ T-cells (right panel, euthanized day 22). (C) Count of IL-10^+ Eμ-TCL1 CLL cells in the spleen of NSG mice without $CD8^+$ T-cells (left, day 17) and with $CD8^+$ T-cells (right, day 22). (D) Count of proliferative ($BrdU^+$) Eμ-TCL1 CLL cells in the spleen of NSG mice without $CD8^+$ T-cells (left, day 17) and with $CD8^+$ T-cells (right, day 22). Statistical comparisons were calculated using one-way ANOVA between matched groups. *p<0.05, **p<0.01, ***p<0.001

Figure 4: Inhibiting CLL IL-10 with $MTM_{ox}32E$ increases the numbers of T- effector cells. Mice were treated as in Figure 3. (A) Frequency of $CD8^+$ T-cells in the blood of NSG mice. (B) (Left) Representative histograms of BrdU incorporation by splenic $CD5^+CD19^-$ T-cells (>99% $CD8^+$). Frequency (middle) and number (right) of $BrdU^+$ splenic $CD8^+$ T-cells. (C) (Left) Representative histograms of IFN-γ production by splenic

CD8$^+$ T-cells. Frequency (middle) and number (right) of splenic IFN-γ$^+$ CD8$^+$ T-cells. (D) Frequency (left) and number (right) of GzB$^+$ CD8$^+$ T-cells in the spleen. (E) Frequency of KLRG1$^+$ highly cytotoxic effector and CD27$^+$ memory CD8$^+$ T-cells in the spleen (left) and pie chart representations of CD8$^+$ T-cell proportions. (F) Frequency of PD-1 expressing CD8$^+$ T-cells in the blood. Statistical comparisons in A+F were obtained by two-way ANOVA comparing vehicle to MTM$_{ox}$32*E* treated mice, and in B-E by one-way ANOVA between vehicle to MTM$_{ox}$32*E*. *p<0.05

Figure 5: Anti-PD-L1 checkpoint blockade is more effective when combined with IL-10 suppression by MTM$_{ox}$32*E*. Three groups of thirteen NSG mice were injected with Eμ-TCL1 and Eμ-TCL1 primed CD8$^+$ T-cells at a ratio of one T cell to 32 CLL cells. Mice received 12mg/kg MTM$_{ox}$32*E* or vehicle every two to three days plus 10mg/kg anti-PD-L1 or isotype control every three days. (A) Frequency of Eμ-TCL1 CLL cells in the blood of NSG mice (mean + SEM). (B-C) Frequency (B) and count (C) of Eμ-TCL1 CLL cells in the spleen. (D) Frequency (left) and count (right) of CD8$^+$ T-cells in the spleen of recipient NSG mice. (E) Frequency of CD8$^+$ T-cells in the blood of NSG recipients (mean + SEM). (F) Frequency (left) and count (right) of Eμ-TCL1 CLL cells in the bone marrow. (G) Percent of mice with less than 30% CLL in the blood over time. Statistical significance in A, E, G was calculated by two-way ANOVA comparing vehicle to treated mice, and by one-way ANOVA comparing vehicle to treated mice in remaining panels. *p<0.05, **p<0.01, ***p<0.001, ****p<0.0001 indicate statistical significance of *difference between combination and ICB alone, #difference between combination and control, &difference between ICB alone and control

Figure 6: Adding IL-10 inhibitor MTM$_{ox}$32*E* to anti-PD-L1 alters CD8+ cell proliferation. Mice were treated as in Figure 5. (A) Frequency of PD-L1$^+$ Eμ-TCL1 CLL

cells in the spleen of NSG mice. (B) Plasma IL-10 levels at euthanasia. (C) Count of $BrdU^+$ splenic $CD8^+$ T-cells. (D) Count of $BrdU^+$ Eμ-TCL1 CLL cells in the spleen. (E) Ratio of total count and count of proliferating $CD8^+$ T-cells to Eμ-TCL1 CLL cells. (F) Correlation between plasma IL-10 levels and total $CD8^+$ T-cell count (left) or proliferating $CD8^+$ T-cell count (right). Graphs show the Pearson's r correlation coefficient, two-tailed p-value, trendline, and 95% confidence interval. Other statistical comparisons were done by one-way ANOVA comparing vehicle to treated mice. *p<0.05, **p<0.01, ***p<0.001, ****p<0.0001

Figure 7: T-cells from Eμ-TCL1 mice are more functional when treated with both anti-PD-L1 checkpoint blockade and IL-10 blockade. Mice were treated as in Figure 5. (A) Frequency of $KLRG1^+$ highly cytotoxic effector and $CD27^+$ memory $CD8^+$ T-cells in the spleen (left) and pie chart representations of $CD8^+$ T-cell proportions. (B-C) Count of IFN-γ^+ (B) and GzB^+ (C) splenic $CD8^+$ T-cells. (D) Frequency of $CD107a^+$ splenic $CD8^+$ T-cells. (E) Gating strategy for $PD1^+CD8^+$ T-cells, and representative histograms showing CTLA4, Lag-3, or Tim-3 expression by $PD1^+CD8^+$ cells. (F-G) Frequency of PD-1^+ $CD8^+$ T-cells (F) and exhausted $CD8^+$ T-cells (double positive for PD-1^+ and either $CTLA4^+$, Lag-3^+, or Tim-3^+) (G) in the spleen. (H) Comparison of CLL frequency in spleen from Figure 5B and Supplemental Figure 4B. (I) Comparison of CLL frequency in the blood from Figures 2F and 5A. Statistical comparisons done by one-way ANOVA comparing vehicle to treated mice, except in H+I where all groups were compared to each other. *p<0.05, **p<0.01, ***p<0.001, ****p<0.0001

Figure 8: Cooperation of IL-10 suppression and checkpoint blockade. Model shows combining IL-10 suppression with anti-PD-L1 ICB enhances antitumor $CD8^+$ T-cell activity by counteracting multiple methods of CLL immune suppression.

Figure 1

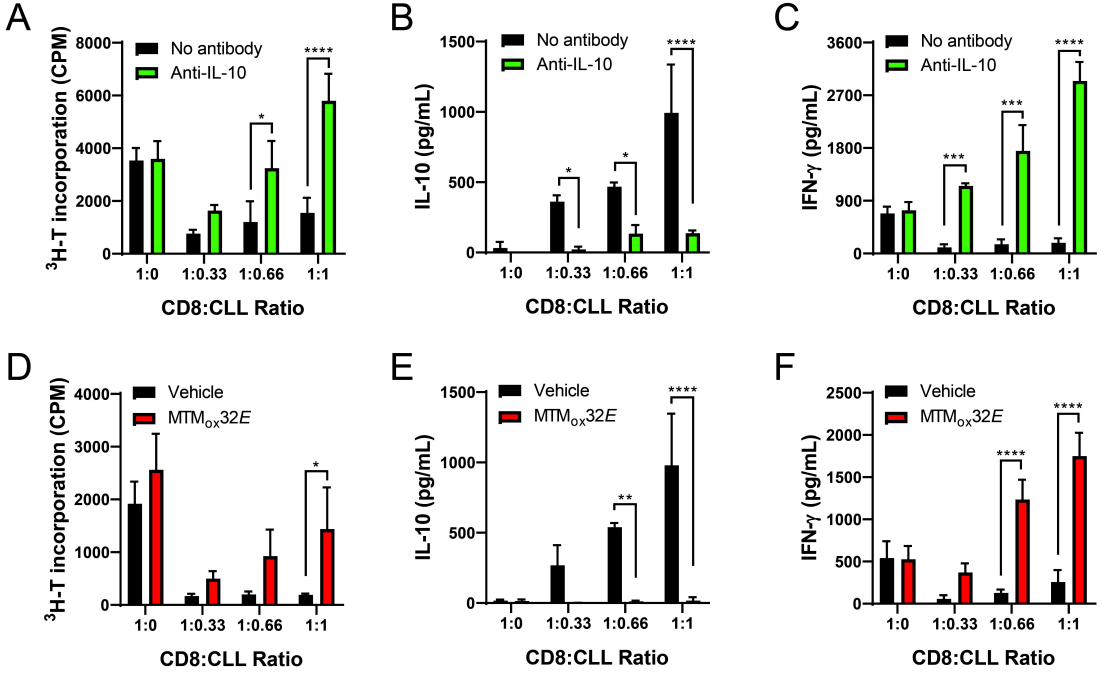
A
No antibody
Anti-IL-10
^{3}H-T incorporation (CPM)
8000
6000
4000
2000
0
1:0
1:0.33
1:0.66
1:1
CD8:CLL Ratio
*
****
B
No antibody
Anti-IL-10
IL-10 (pg/mL)
1500
1000
500
0
1:0
1:0.33
1:0.66
1:1
CD8:CLL Ratio
*
*
****
C
No antibody
Anti-IL-10
IFN-γ (pg/mL)
3600
2700
1800
900
0
1:0
1:0.33
1:0.66
1:1
CD8:CLL Ratio
***
***
****
D
Vehicle
MTM$_{ox}$32*E*
^{3}H-T incorporation (CPM)
4000
3000
2000
1000
0
1:0
1:0.33
1:0.66
1:1
CD8:CLL Ratio
*
E
Vehicle
MTM$_{ox}$32*E*
IL-10 (pg/mL)
1500
1000
500
0
1:0
1:0.33
1:0.66
1:1
CD8:CLL Ratio
**
****
F
Vehicle
MTM$_{ox}$32*E*
IFN-γ (pg/mL)
2500
2000
1500
1000
500
0
1:0
1:0.33
1:0.66
1:1
CD8:CLL Ratio
****
****

Figure 2

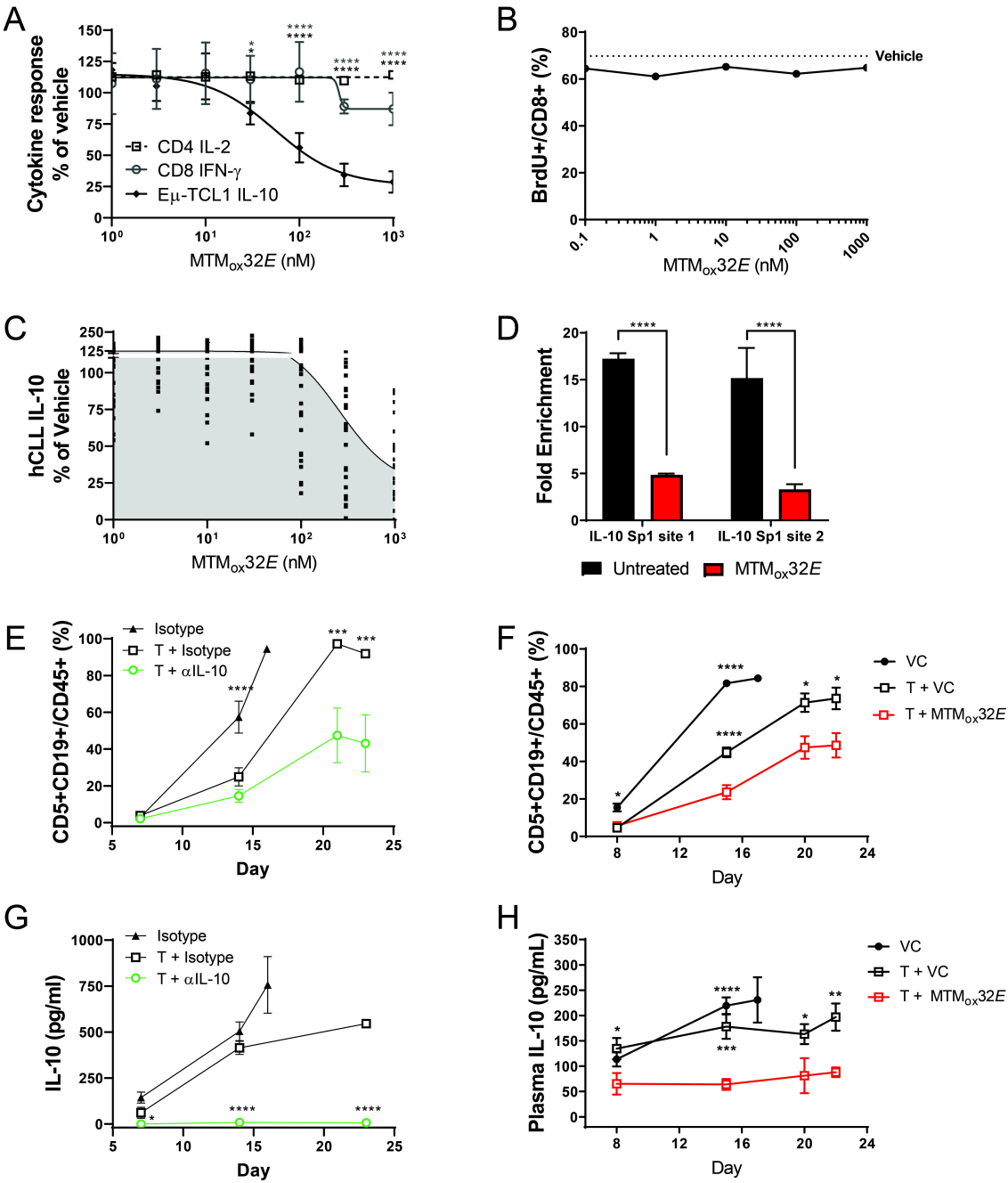
A
Cytokine response % of vehicle
CD4 IL-2
CD8 IFN-γ
Eμ-TCL1 IL-10
MTMox32E (nM)
B
BrdU+/CD8+ (%)
Vehicle
MTMox32E (nM)
C
hCLL IL-10 % of Vehicle
MTMox32E (nM)
D
Fold Enrichment
IL-10 Sp1 site 1
IL-10 Sp1 site 2
Untreated
MTMox32E
E
CD5+CD19+/CD45+ (%)
Isotype
T + Isotype
T + αIL-10
Day
F
CD5+CD19+/CD45+ (%)
VC
T + VC
T + MTMox32E
Day
G
IL-10 (pg/ml)
Isotype
T + Isotype
T + αIL-10
Day
H
Plasma IL-10 (pg/mL)
VC
T + VC
T + MTMox32E
Day

Figure 3

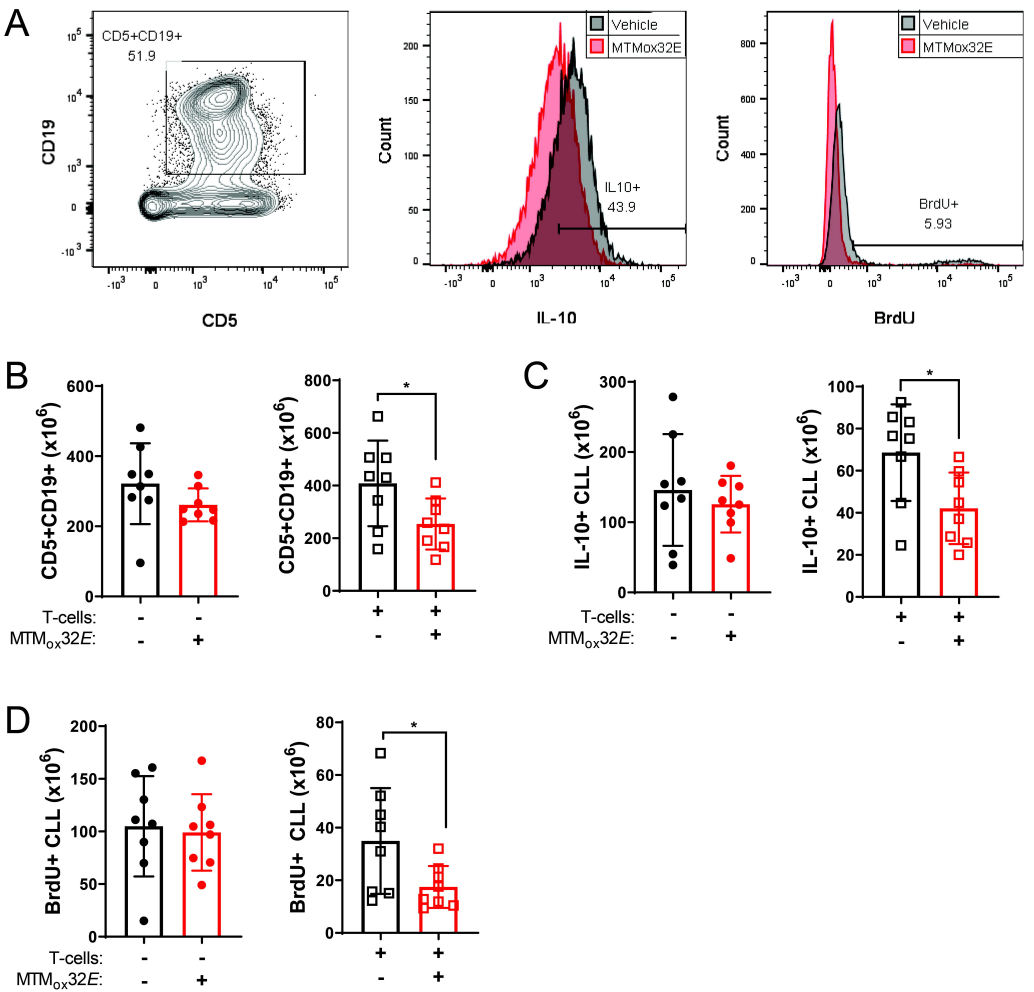
A
CD5+CD19+
51.9
CD19
CD5
Vehicle
MTMox32E
Count
IL10+
43.9
IL-10
Vehicle
MTMox32E
Count
BrdU+
5.93
BrdU
B
CD5+CD19+ (x10^6)
T-cells:
MTMox32E:
CD5+CD19+ (x10^6)
*
C
IL-10+ CLL (x10^6)
T-cells:
MTMox32E:
IL-10+ CLL (x10^6)
*
D
BrdU+ CLL (x10^6)
T-cells:
MTMox32E:
BrdU+ CLL (x10^6)
*

Figure 4

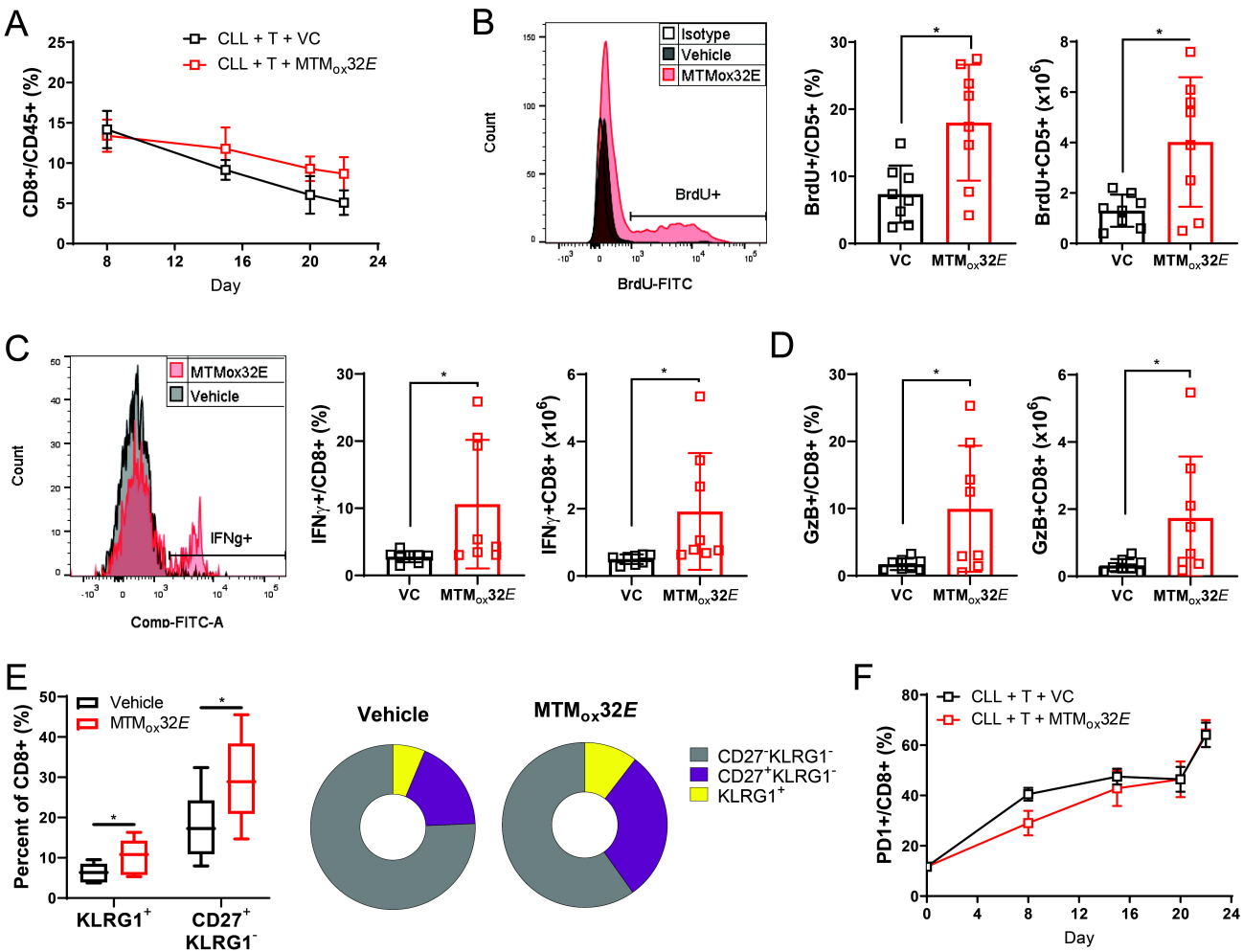
A
CLL + T + VC
CLL + T + MTMox32E
CD8+/CD45+ (%)
Day
B
Isotype
Vehicle
MTMox32E
Count
BrdU+
BrdU-FITC
BrdU+/CD5+ (%)
BrdU+CD5+ (x10^6)
VC
MTMox32E
C
MTMox32E
Vehicle
Count
IFNg+
Comp-FITC-A
IFNγ+/CD8+ (%)
IFNγ+CD8+ (x10^6)
D
GzB+/CD8+ (%)
GzB+CD8+ (x10^6)
E
Vehicle
MTMox32E
Percent of CD8+ (%)
KLRG1+
CD27+ KLRG1-
CD27-KLRG1-
CD27+KLRG1-
KLRG1+
F
CLL + T + VC
CLL + T + MTMox32E
PD1+/CD8+ (%)
Day

Figure 5

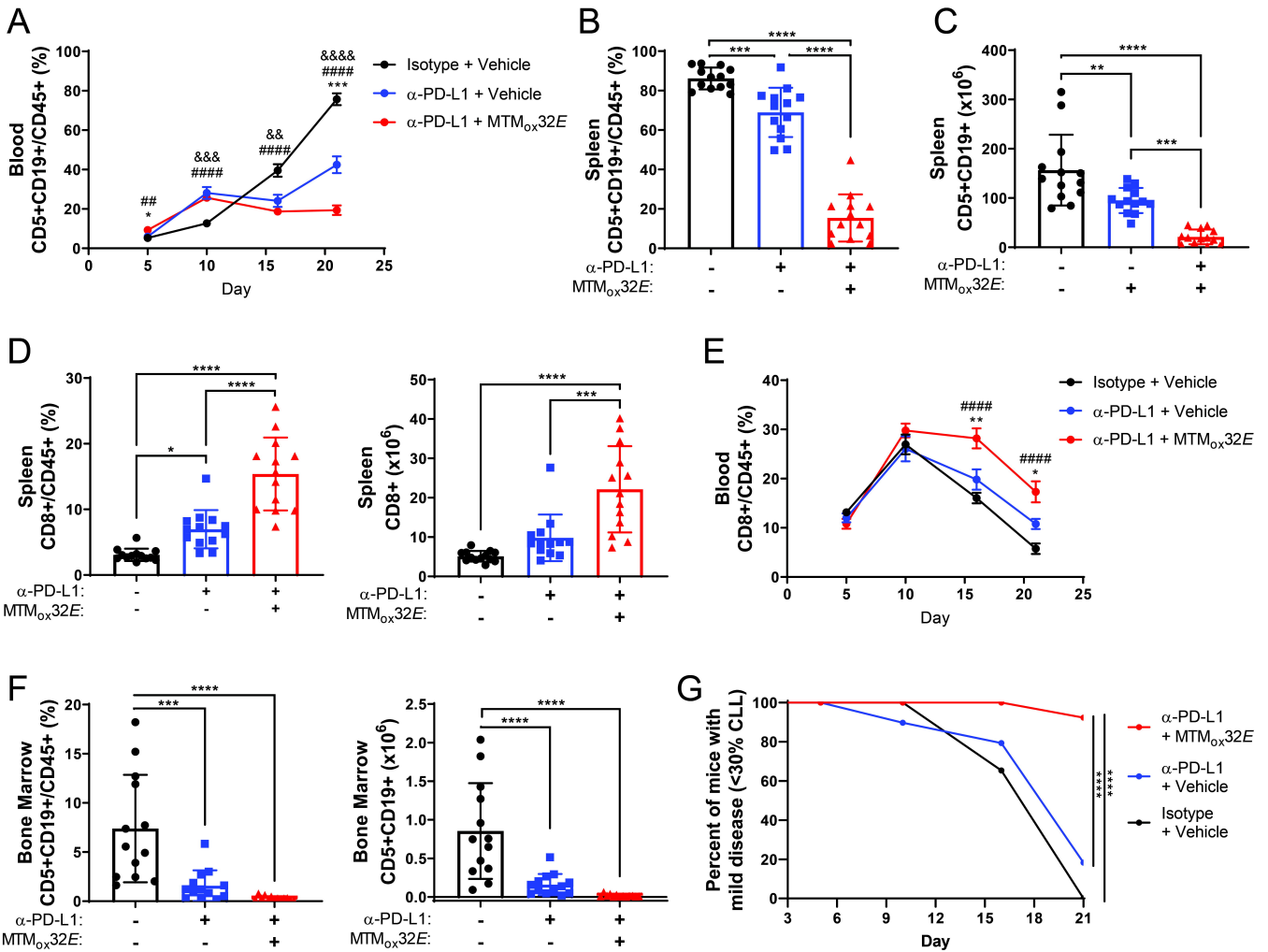
A
Blood
CD5+CD19+/CD45+ (%)
Day
Isotype + Vehicle
α-PD-L1 + Vehicle
α-PD-L1 + MTMox32E
B
Spleen
CD5+CD19+/CD45+ (%)
α-PD-L1:
MTMox32E:
C
Spleen
CD5+CD19+ (x10^6)
α-PD-L1:
MTMox32E:
D
Spleen
CD8+/CD45+ (%)
Spleen
CD8+ (x10^6)
α-PD-L1:
MTMox32E:
E
Blood
CD8+/CD45+ (%)
Day
Isotype + Vehicle
α-PD-L1 + Vehicle
α-PD-L1 + MTMox32E
F
Bone Marrow
CD5+CD19+/CD45+ (%)
Bone Marrow
CD5+CD19+ (x10^6)
α-PD-L1:
MTMox32E:
G
Percent of mice with
mild disease (<30% CLL)
Day
α-PD-L1
+ MTMox32E
α-PD-L1
+ Vehicle
Isotype
+ Vehicle

Figure 6

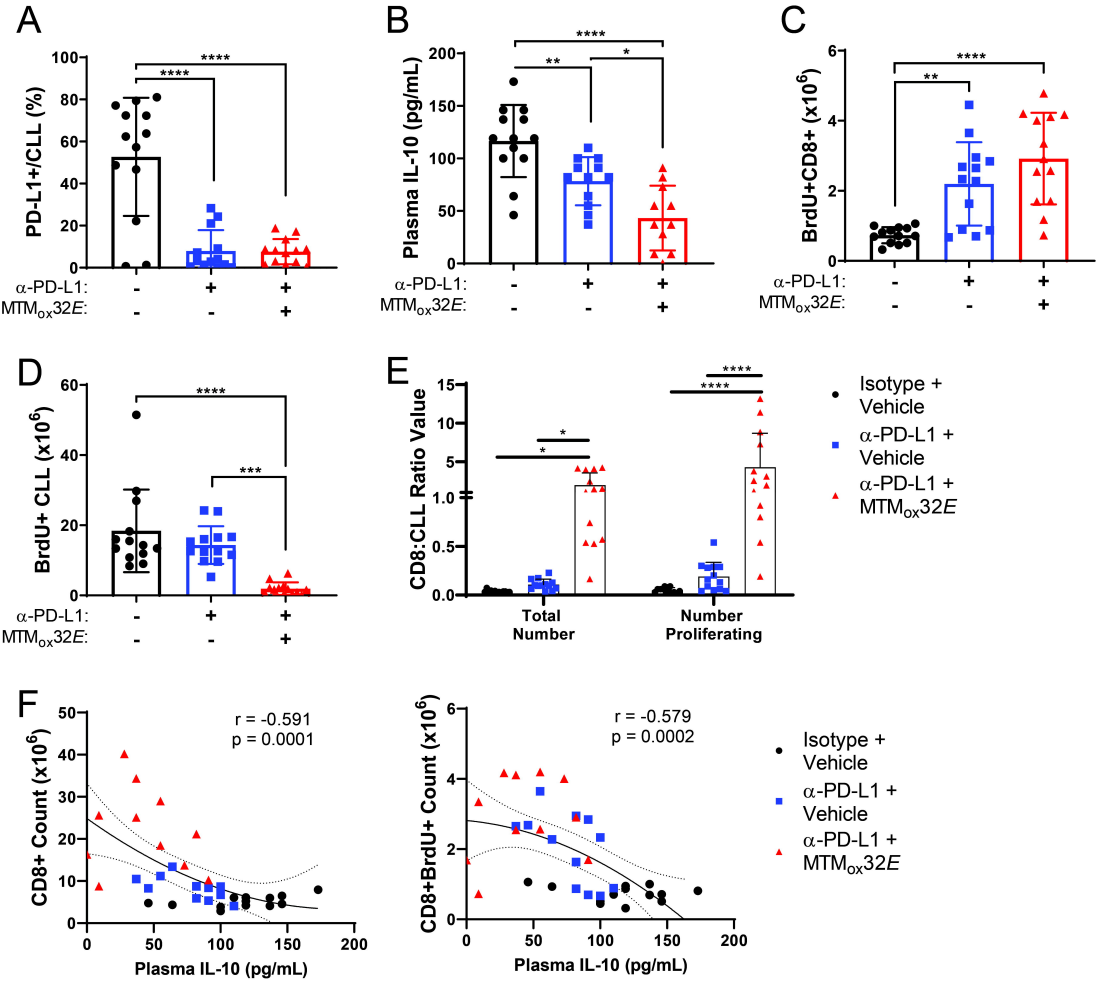
A
PD-L1+/CLL (%)
α-PD-L1:
MTMox32E:
B
Plasma IL-10 (pg/mL)
C
BrdU+CD8+ (x10^6)
D
BrdU+ CLL (x10^6)
E
CD8:CLL Ratio Value
Total Number
Number Proliferating
Isotype + Vehicle
α-PD-L1 + Vehicle
α-PD-L1 + MTMox32E
F
CD8+ Count (x10^6)
r = -0.591
p = 0.0001
Plasma IL-10 (pg/mL)
CD8+BrdU+ Count (x10^6)
r = -0.579
p = 0.0002

Figure 7

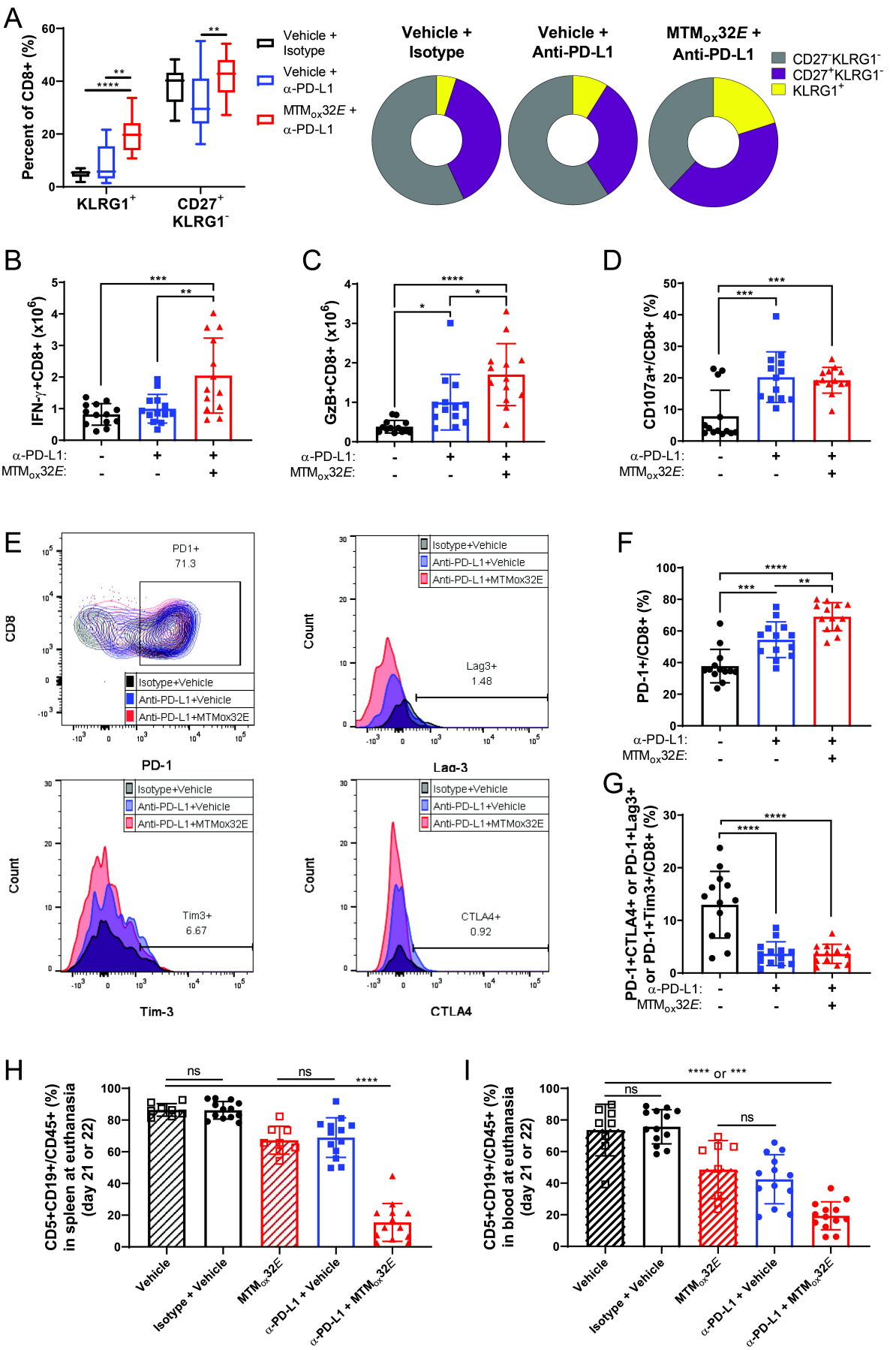
A
Percent of CD8+ (%)
KLRG1+
CD27+ KLRG1-
Vehicle + Isotype
Vehicle + α-PD-L1
MTMox32E + α-PD-L1
Vehicle + Isotype
Vehicle + Anti-PD-L1
MTMox32E + Anti-PD-L1
CD27-KLRG1-
CD27+KLRG1-
KLRG1+
B
IFN-γ+CD8+ (x10^6)
C
GzB+CD8+ (x10^6)
D
CD107a+/CD8+ (%)
α-PD-L1:
MTMox32E:
E
PD1+
71.3
CD8
PD-1
Isotype+Vehicle
Anti-PD-L1+Vehicle
Anti-PD-L1+MTMox32E
Count
Lag3+
1.48
Lag-3
Tim3+
6.67
Tim-3
CTLA4+
0.92
CTLA4
F
PD-1+/CD8+ (%)
G
PD-1+CTLA4+ or PD-1+Lag3+ or PD-1+Tim3+/CD8+ (%)
H
CD5+CD19+/CD45+ (%) in spleen at euthanasia (day 21 or 22)
ns
Vehicle
Isotype + Vehicle
MTMox32E
α-PD-L1 + Vehicle
α-PD-L1 + MTMox32E
I
CD5+CD19+/CD45+ (%) in blood at euthanasia (day 21 or 22)
**** or ***

Figure 8

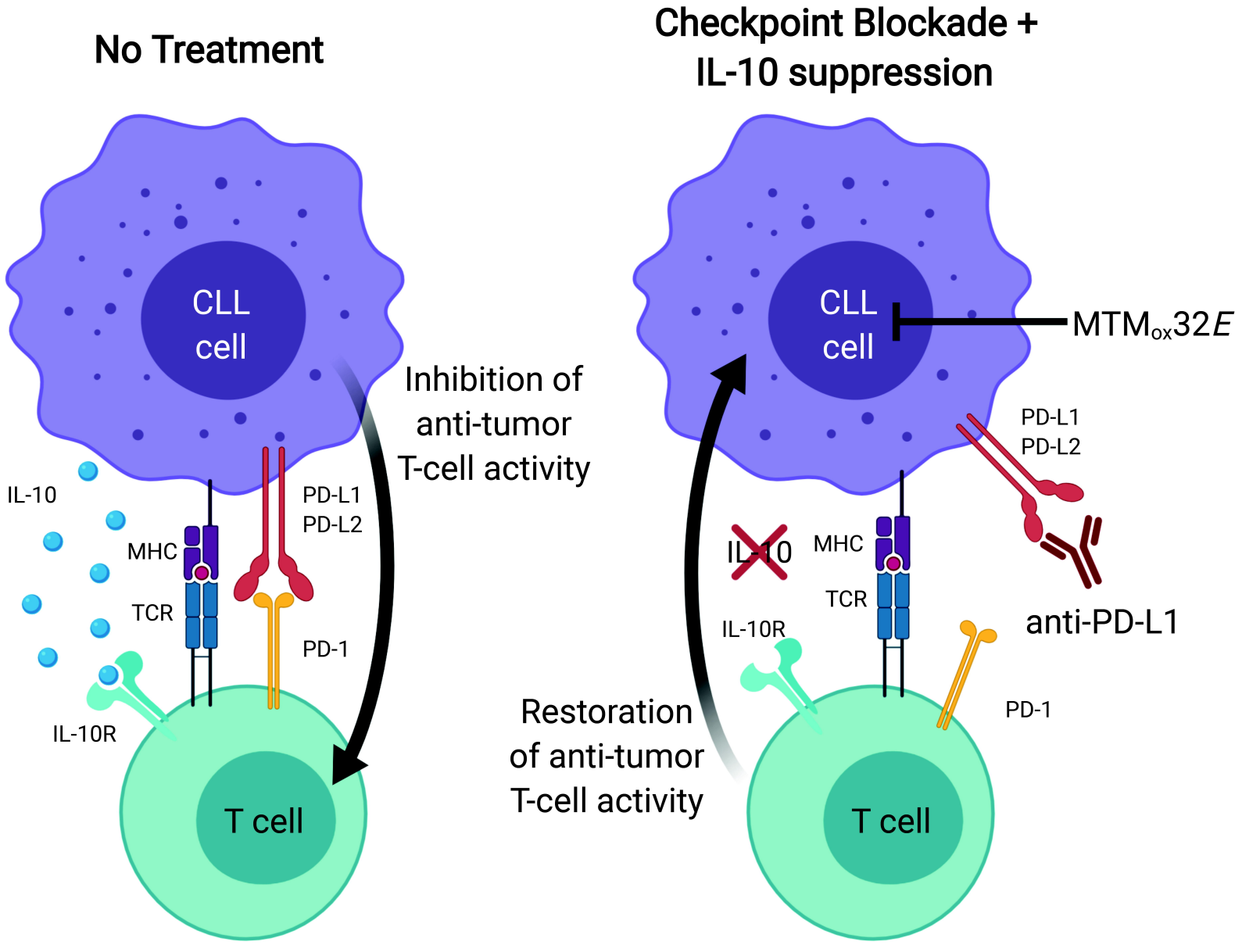
No Treatment
CLL cell
IL-10
MHC
TCR
PD-L1
PD-L2
PD-1
IL-10R
T cell
Inhibition of anti-tumor T-cell activity
Checkpoint Blockade + IL-10 suppression
CLL cell
MTMox32E
PD-L1
PD-L2
IL-10
MHC
TCR
IL-10R
anti-PD-L1
PD-1
T cell
Restoration of anti-tumor T-cell activity